



OPEN ACCESS

EDITED BY

Efthalia Chatzisymeon,
University of Edinburgh, United Kingdom

REVIEWED BY

Jing Zou,
Huaqiao University, China
Yuqiong Gao,
University of Shanghai for Science and
Technology, China

*CORRESPONDENCE

Sanja J. Armaković,
✉ sanja.armakovic@dh.uns.ac.rs

SPECIALTY SECTION

This article was submitted to Water and
Wastewater Management,
a section of the journal
Frontiers in Environmental Science

RECEIVED 13 December 2022

ACCEPTED 23 January 2023

PUBLISHED 07 February 2023

CITATION

Bilić A, Savanović MM, Armaković S,
Četojević-Simin DD, Srđenović Čonić B,
Kladar N and Armaković SJ (2023),
Exploring the influence of free radicals on
photolytic removal of nadolol from water:
Mechanism of degradation and toxicity
of intermediates.
Front. Environ. Sci. 11:1119944.
doi: 10.3389/fenvs.2023.1119944

COPYRIGHT

© 2023 Bilić, Savanović, Armaković,
Četojević-Simin, Srđenović Čonić, Kladar
and Armaković. This is an open-access
article distributed under the terms of the
[Creative Commons Attribution License
\(CC BY\)](https://creativecommons.org/licenses/by/4.0/). The use, distribution or
reproduction in other forums is permitted,
provided the original author(s) and the
copyright owner(s) are credited and that
the original publication in this journal is
cited, in accordance with accepted
academic practice. No use, distribution or
reproduction is permitted which does not
comply with these terms.

Exploring the influence of free radicals on photolytic removal of nadolol from water: Mechanism of degradation and toxicity of intermediates

Andrijana Bilić¹, Maria M. Savanović^{1,2}, Stevan Armaković^{2,3},
Dragana D. Četojević-Simin⁴, Branislava Srđenović Čonić^{5,6},
Nebojša Kladar^{5,6} and Sanja J. Armaković^{1,2*}

¹University of Novi Sad, Faculty of Sciences, Department of Chemistry, Biochemistry and Environmental Protection, Novi Sad, Serbia, ²Association for the International Development of Academic and Scientific Collaboration—AIDASCO, Novi Sad, Serbia, ³University of Novi Sad, Faculty of Sciences, Department of Physics, Novi Sad, Serbia, ⁴Department of Pharmacy, Singidunum University, Belgrade, Serbia, ⁵University of Novi Sad, Faculty of Medicine, Department of Pharmacy, Novi Sad, Serbia, ⁶University of Novi Sad, Faculty of Medicine, Center for Medical and Pharmaceutical Investigations and Quality Control, Novi Sad, Serbia

β -blockers are known to have negative effects on fish and other aquatic animal species, so their removal is key for preserving aquatic ecosystems. To reduce the risks related to β -blockers, it is necessary to assess their effects and develop more effective treatments such as advanced oxidation processes. Improving sewage treatments is a critical approach to reducing β -blockers in aquatic environments. In this work, for the first time, the direct and indirect photolysis of nadolol (NAD) was investigated under different light sources (simulated solar (SS), UV-LED, and UV radiations) in ultrapure water. Indirect photolysis by H_2O_2 showed 1.5, 2.1, and 5.6 times higher NAD degradation efficiency than direct photolysis under mentioned irradiations. This effect was particularly pronounced in the presence of UV radiation, in which the degradation efficiency of NAD was the highest (80.2%). Computational analysis based on density functional theory calculations, together with the results of NAD photodegradation efficiency in the presence of radical scavengers (isopropanol and benzoquinone), was used to propose the NAD degradation mechanism. Sixteen degradation intermediates were proposed, along with their NMR chemical shifts. Also, this study analyzed the degree of catalase activity, lipid peroxidation, and hydroxyl radicals neutralization of NAD and its photodegradation mixtures obtained after indirect photolysis. The degree of mineralization and *in vitro* toxicity of NAD and its degradation intermediates obtained in the presence of UV/ H_2O_2 were assessed.

KEYWORDS

indirect photolysis, DFT, density functional theory, catalase activity, lipid peroxidation, human cell lines

1 Introduction

Although pharmaceuticals are developed to improve human health, their excessive use worldwide and the fact that they are active at low concentrations have made them one of the emerging pollutants in the environment (Wols et al., 2013). Pharmaceuticals have been detected at low concentrations in wastewater, surface water, and groundwater in Europe, the USA, and

Canada (Carlson et al., 2015). If the drinking water is produced from surface water, pharmaceuticals can even be detected in tap water at concentrations of ng/L. Still, there is currently a shortage of information about the long-term effects of exposure on human health. One of the primary reasons pharmaceuticals appear in natural waters is the ineffectiveness of conventional wastewater treatment plants (WWTP) (Svendsen et al., 2020). WWTPs are designed to remove and degrade simple to slightly complex chemicals, such as biodegradable carbon, nitrogen, and phosphorus compounds, along with microorganisms, nutrients, and pathogens, but not persistent micropollutants such as pharmaceuticals (Khasawneh and Palaniandy, 2021).

Beta-blockers are among the widely consumed pharmaceuticals prescribed for cardiovascular diseases and treat disorders such as angina, hypertension, arrhythmias, and long-term use after a heart attack (Wang et al., 2012). Due to the increased prevalence of cardiopathy and hypertension, the global market value and the number of beta-blockers prescriptions keep increasing yearly (Ye et al., 2022). Nadolol (NAD) is a commonly used beta-blocker whose percentage excreted in urine is 24.6%. Since it, like most pharmaceuticals, is not removed efficiently enough from wastewater, it is not surprising that its presence was detected in natural water at a concentration of 0.062 µg/L (Yi et al., 2020). Maszkowska et al. investigated the hydrolytic stability of NAD in water, and the results showed high stability. His half-life in the aquatic environment at 25°C was more than one year (Maszkowska et al., 2014).

Direct and indirect photolysis is a crucial way of degrading pharmaceuticals in the environment. According to direct photolysis, the organic compounds are degraded using photon attack. The UV spectrum of β -blockers shows that most compounds from this group absorb only radiation in the UVC region (Piram et al., 2008), which is why they do not degrade in water through direct photolysis to the extent that would prevent the accumulation in the environment. Various emerging methods have been studied to remove organic contaminants from water in recent years, such as biological treatment (Liu et al., 2020), chemical oxidation using ozone (Gomes et al., 2020), membrane filtration (Li et al., 2022a), and activated carbon adsorption (Zhan et al., 2022). These available technologies have some disadvantages compared to direct and indirect photolysis. For example, adsorption techniques will create secondary pollution by simply transferring the contaminants from one phase to another. It is well known that UV irradiation of H_2O_2 in aqueous solutions leads to the production of hydroxyl radical ($\cdot\text{OH}$), an oxidant with a high oxidation potential. It can oxidize many different organic and inorganic substrates under very mild conditions in a wide range of pH values (Guo et al., 2022). UV/ H_2O_2 photodegradation is the most attractive, efficient, and environmentally friendly way of decomposing organic micropollutants (Khorsandi et al., 2019). A minor disadvantage of photolysis under UV irradiation is using Mercury lamps as a radiation source. In recent years, UV-LED has gained considerable attention as an alternative radiation source because it has a long lifetime and is mercury-free (Fujioka et al., 2020). In industry, H_2O_2 is used as an effective bleach instead of chlorine-containing agents. From an environmental point of view, H_2O_2 is very suitable for use since it only produces H_2O and O_2 during degradation, which makes it one of the cleanest and most readily available oxidizing agents.

According to the available literature, the kinetics and efficiency of direct and indirect photolysis of NAD in water in the presence of H_2O_2 under simulated solar (SS), UV-LED, and UV radiations were examined for the first time in this work. The degree of catalase

activity, lipid peroxidation, and hydroxyl radicals neutralization of NAD and its photodegradation mixtures obtained during indirect photolysis were analyzed. Density functional theory (DFT) calculations have been performed to investigate the reactive properties of NAD with $\cdot\text{OH}$ radical. Reaction intermediates were proposed based on the influence of radical scavengers on the removal efficiency of NAD, as well as computational simulations. The degree of mineralization and chemical oxygen demand (COD) were determined after 180 min. *In vitro* toxicity of the parent compound and mixtures of degradation intermediates formed was assessed using human cell lines colon adenocarcinoma HT-29 and fetal lung MRC-5.

An increasing number of research groups are working on elucidating the degradation mechanisms under UV/ H_2O_2 , which shows how important these processes are. The primary reason is simplicity and efficiency compared to direct photolysis.

2 Materials and methods

2.1 Chemicals and solutions

All chemicals used in the experiments were reagent grade and were utilized without further purification. The pharmaceutical NAD ((2R, 3S)-5-[3-(tert-butylamino)-2-hydroxypropoxy]-1,2,3,4-tetrahydronaphthalene-2,3-diol, $\text{C}_{17}\text{H}_{27}\text{NO}_4$, $M = 309.4$ g/mol, $\geq 99\%$ purity, Sigma-Aldrich, Germany), and chemicals H_2O_2 (30%, Sigma-Aldrich, Germany) isopropanol (IPA, $\geq 98\%$, Sigma-Aldrich, Germany) and benzoquinone (BQ, $\geq 98\%$, Sigma-Aldrich, Germany) were used in this work. More information about applied chemicals is given in the [Supplementary material](#).

2.2 Degradation procedures

Experiments were performed using 20 mL of 0.05 mmol/L NAD. In the indirect photolysis experiments, the solution contained 3.0 mmol/L of H_2O_2 . The solution was irradiated for 180 min. The SS irradiation source was a 50 W halogen lamp (Philips, with the intensity of 1.9×10^{-2} W/cm² in the visible region and 4.5×10^{-5} W/cm² in the UV region), and the UV-LED radiation source was a 5 W UV-LED Lamp (Enjoydeal, China, type: MR16 AC 85-265V/12, with intensity of 2.3×10^{-3} W/cm² in the visible region, and 2.2×10^{-4} W/cm² in the UV region). As the UV radiation source, a 125 W high-pressure Mercury lamp was used (Philips, HPL-N, emission bands at 290, 293, 296, 304, 314, 335, and 366 nm, with maximum emission at 366 nm and intensity of 5.0×10^{-3} W/cm² in the visible region and 1.6×10^{-3} W/cm² in the UV region). More information about energy fluxes measurement is given in [Supplementary material](#).

All experiments were performed at the natural pH without any adjustment (c.a. 8.0), which declines during the photodegradation ([Supplementary Table S1](#)). To investigate the degradation mechanism, reactive radicals scavengers (2.0 mmol/L IPA or BQ) have been added to a water solution of NAD/ H_2O_2 .

2.3 Analytical procedures

For monitoring of kinetics of NAD photodegradation, aliquots of 0.40 mL were taken from the reaction mixture at the beginning of the

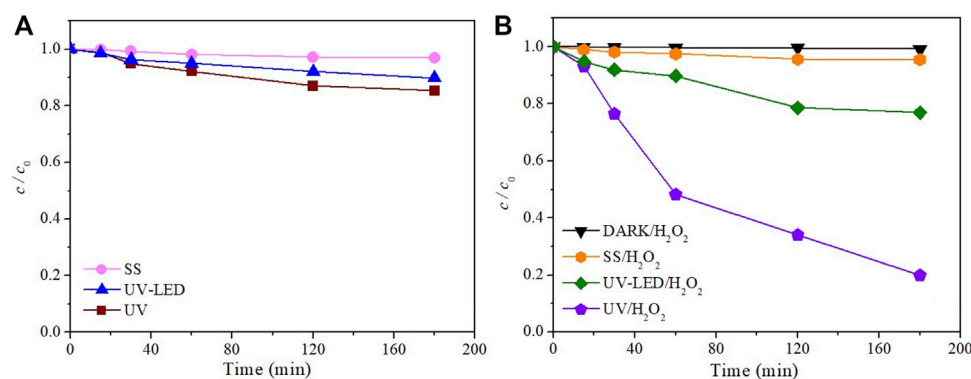


FIGURE 1

The kinetics of NAD degradation (0.05 mmol/L) (A) in the absence and (B) presence of 3 mmol/L H_2O_2 under different irradiation sources (temperature $25^\circ C \pm 1^\circ C$, flow rate of O_2 3.0 L/min).

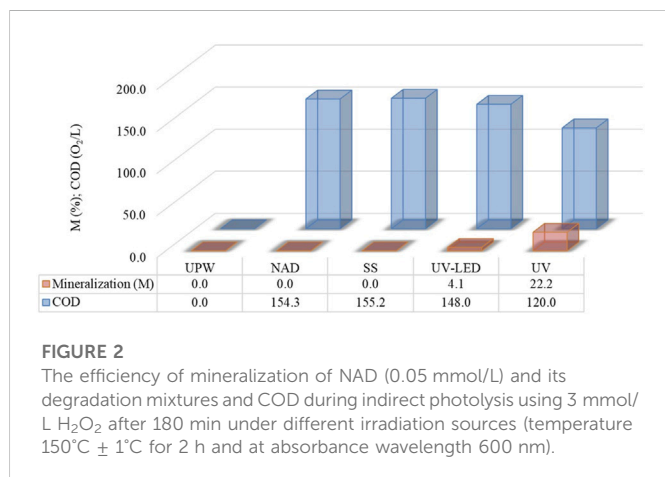


FIGURE 2

The efficiency of mineralization of NAD (0.05 mmol/L) and its degradation mixtures and COD during indirect photolysis using 3 mmol/L H_2O_2 after 180 min under different irradiation sources (temperature $150^\circ C \pm 1^\circ C$ for 2 h and at absorbance wavelength 600 nm).

experiment and at regular time intervals. A 20 μL sample was injected and analyzed using Ultra Fast Liquid Chromatography with Diode Array Detection (UFLC–PDA, Shimadzu), equipped with an Eclipse XDB–C18 column (150 mm \times 4.6 mm i.d., particle size 5 μm , $30^\circ C$). The UV/Vis PDA detector was set at 210 nm (wavelength of maximum absorption of NAD). Experimental conditions for the UFLC–DA can be found in the [Supplementary material](#).

Absorption spectra of NAD was recorded on a double-beam T80+UV/Vis Spectrometer (UK) at a fixed slit width (2 nm), using a quartz cell (1 cm optical length) and computer-loaded UV Win 5 data software. The absorption maximum of NAD was 210 nm ([Supplementary Figure S1](#)).

During the degradation process, a combination glass electrode (pH-Electrode SenTix 20, WTW) connected to a pH meter (pH/Cond 340i, WTW) was used to track the initial pH values and how they changed over time ([Supplementary Table S1](#)).

The degree of hydroxyl radicals neutralization obtained by Fenton's reaction was measured as the ability of hydroxyl radicals to induce lipid peroxidation of liposomal unsaturated fatty acids, followed by the formation of a colored adduct between malondialdehyde and thiobarbituric acid at 532 nm ([Kladar et al., 2015](#)). Catalase activity was measured after incubation (1 h at $37^\circ C$) of 100 μL of heparinized blood and 200 μL of analyzed samples ([Jelić et al., 2018](#)). The reduction rate of H_2O_2 was followed at 240 nm for 3 min at $25^\circ C$, and the percentage

of catalase activity was calculated. The lipid peroxidation process in heparinized blood incubated with investigated samples was determined according to the previously described liquid chromatography based analytical method ([Khoschsorur et al., 2000](#)).

The COD concentration was measured using spectrometry by measuring the absorbance of the formed Cr^{+3} at 600 nm. Absorbance was measured on a double-beam T80+UV-Vis. The samples were digested at $150^\circ C$ for 2 h.

The *in vitro* toxicity effects were assessed using the human cell lines colon adenocarcinoma HT-29 (ECACC 91072201) and fetal lung MRC-5 (ECACC 05090501). Cell growth was evaluated by the colorimetric sulforhodamine B (SRB) assay, according to [Skehan et al. \(1990\)](#), modified by [Četojević-Simin et al. \(2013\)](#). The effect on cell growth was calculated as $(A_t/A_c) \times 100$ [%], where A_t is the absorbance of the test sample and A_c is the absorbance of the control. The experimental details about the cell growth activity are described in [Supplementary material](#).

2.4 Computational details

DFT calculations have been performed using the B3LYP density functional in combination with 6-31G (d,p) basis set ([Ditchfield et al., 1971](#); [Vosko et al., 1980](#); [Lee et al., 1988](#); [Becke, 1993](#); [Stephens et al., 1994](#); [Rassolov et al., 1998](#); [Rassolov et al., 2001](#)). All molecules were subjected to frequency calculations to check that geometrical optimizations identified the true ground states ([Supplementary Figure S2](#)). During geometrical optimizations, frequency and property calculations, the effects of water were taken into account in the framework of the Poisson-Boltzmann solver. DFT calculations were performed with the Jaguar program ([Bochevarov et al., 2013](#); [Cao et al., 2016](#); [Jacobson et al., 2017](#); [Cao et al., 2021](#)), as implemented in the Schrödinger Materials Science Suite 2022-2. NMR chemical shifts were also obtained *via* DFT calculations, according to the approach described in the paper by [Cao et al. \(2005\)](#). Before geometrical optimizations *via* the DFT approach, the initial structure of NAD was pre-optimized using the GFN2-xTB method ([Grimme et al., 2017](#); [Bannwarth et al., 2019](#); [Pracht et al., 2019](#); [Bannwarth et al., 2021](#)), as implemented in the xtb program, developed by the group of Prof. Grimme. GFN2-xTB calculations were performed by implicitly including the influence of water as the solvent in the framework of the Analytical Linearized Poisson-Boltzmann

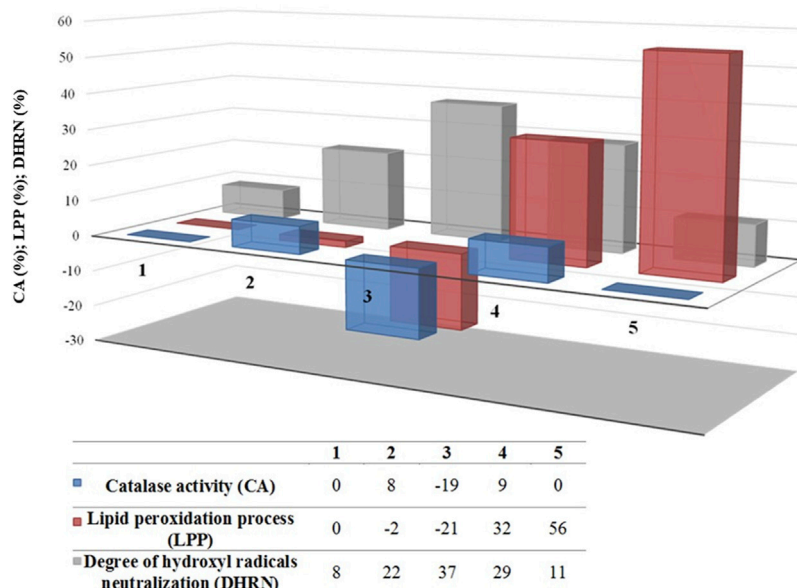


FIGURE 3

Degree of catalase activity, lipid peroxidation, and $\cdot\text{OH}$ radicals neutralization in the presence of (1) UPW, (2) NAD (0.05 mmol/L), and photodegradation mixtures obtained in the presence of H_2O_2 (3 mmol/L) under (3) SS, (4) UV-LED, and (5) UV.

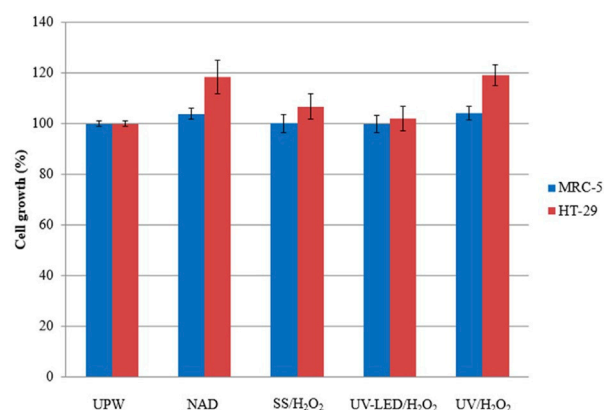


FIGURE 4

Effect of UPW, solution of NAD (0.05 mmol/L) and its photodegradation mixtures obtained by indirect photolysis in the presence of H_2O_2 (3 mmol/L) on the selected human cell lines *in vitro*.

(ALPB) model (Ehlert et al., 2021). Calculations with xtb program were performed *via* the online molecular modeling platform atomistica.online, available at <https://atomistica.online> Armaković and Armaković (2022).

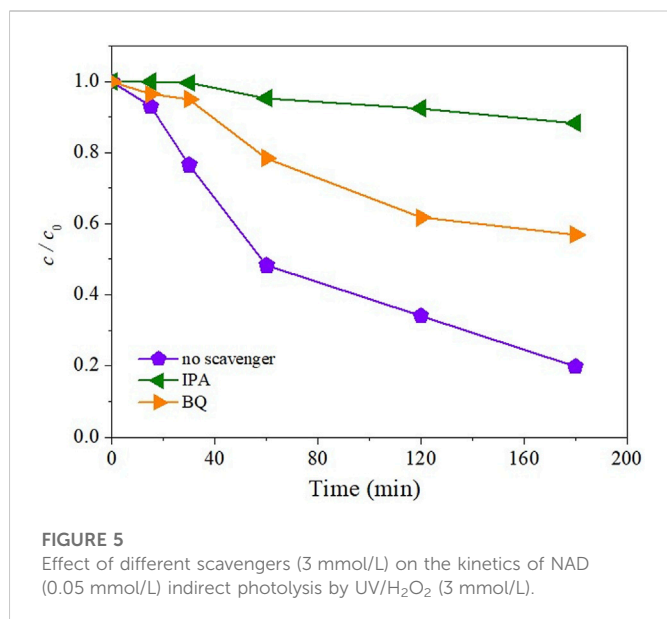
3 Results and discussion

3.1 Removal of nadolol and its degradation intermediates from water

If the degradation results are compared under the influence of different radiation sources (Figure 1), significantly higher efficiency is

observed during degradation under UV radiation than degradation along SS and UV-LED. After 180 min, 3.0% and 11.0% of NAD were degraded under SS and UV-LED radiation, respectively (Figure 1A). The degradation efficiency was slightly higher using UV radiation, wherein 14.7% of the NAD was degraded for the same time. The obtained results are expected considering that absorptive peaks of NAD are at 210 and 274 nm, which contributes to a higher degradation efficiency by applying a high-pressure Mercury lamp than a halogen lamp. For effective direct photolysis, there must be an appropriate overlap between the investigated compound absorption spectrum (Supplementary Figure S1) and the corresponding radiation source spectrum (Bonvin et al., 2013). Fujioka et al. (2020) have determined that UV-LED irradiation sources are less effective than UV irradiation sources for degrading organic compounds with absorption maximums in the UV area due to the longer emission wavelengths of the UV-LED lamps.

To increase the degradation efficiency of NAD, indirect photolysis in the presence of H_2O_2 has been investigated under SS, UV-LED, and UV radiation. H_2O_2 , as an oxidant with a high oxidation potential, can oxidize many different organic and inorganic substrates under very mild conditions in a wide range of pH values (Goyal et al., 2020). The obtained results show that in comparison to the direct photolysis of NAD, adding H_2O_2 increased degradation efficiency under all three types of irradiation (Figure 1B). Further, indirect photolysis of NAD was the most efficient under UV radiation, whereby 80.2% of NAD was degraded. Lower degradation efficiency was achieved under UV-LED and SS irradiation, where 23.1% and 4.5% of NAD were degraded after 180 min, respectively. It is well known that UV irradiation of H_2O_2 in aqueous solutions leads to the production of $\cdot\text{OH}$, and other reactive species, such as $\text{O}_2^{\cdot-}$ since H_2O_2 absorbs light in the 185–300 nm range. These radicals react with the substrate, forming intermediates that further react with $\cdot\text{OH}$ radicals until complete mineralization. $\cdot\text{OH}$ radicals are short-lived and highly reactive



chemical species that indiscriminately react with NAD and its intermediates in water. $\bullet\text{OH}$ radical's action mechanism on NAD consists of several processes: elimination of hydrogen, electrophilic bonding, and electron transfer. Therefore, the higher degradation efficiency of NAD in the presence of UV-LED/H₂O₂ and UV/H₂O₂ was anticipated.

The initial pH value of the NAD solution under UV is 8.2. During direct degradation by photolysis, the value increases to 9.2 (Supplementary Table S1), probably due to the formation of slightly basic intermediates concerning the starting compound. The initial pH value of the solution was somewhat lower in the presence of H₂O₂ than in pure NAD solution. During indirect photolysis, the pH value of the solution constantly decreases, most likely due to the formation of slightly acid intermediates in the starting compound. A similar trend is after 180 min indirect photolysis, the value decreases from 7.7 to 6.8.

Many organic compounds are mineralized during UV/H₂O₂ treatment since $\bullet\text{OH}$ radicals are non-selective, highly reactive species (Lopez-Alvarez et al., 2016; Ghanbari et al., 2021; Santolin et al., 2022). The final products include CO₂, H₂O, and inorganic ions. However, it is crucial to know that high mineralization levels are rarely reached since organic compounds, such as pharmaceuticals, are very stable in water. The mineralization of investigated solutions for different degradation processes, shown as COD measurements, determined that 4.1% and 22.2% of NAD and its degradation intermediates were removed after 180 min under UV-LED and UV irradiation (Figure 2). Based on the presented results, we can conclude that the UV/H₂O₂ treatment proved to be effective in the case of NAD degradation but not in the case of its intermediates. (Figures 1, 2).

After 180 min of UV irradiation, the content of organic intermediates in the suspension was approximately 78%. The difference in the efficiency obtained based on COD and UFLC-DAD determination results from forming various aromatic and aliphatic intermediates, considering that UFLC monitors only the NAD. The COD method monitors intermediates that arise from indirect photolysis. Also, it may be inferred that a mixture of NAD

and its organic intermediates formed under UV-LED radiation are stable and not subject to decomposition under the mentioned radiation sources.

Based on the obtained results, we can conclude that the degradation of NAD is accompanied by the formation of intermediates, especially under UV irradiation, that can potentially harm the environment. Having that in mind, it is essential to identify them and evaluate reactivity and toxicity.

3.2 Assessment of reactivity and toxicity of NAD and its degradation intermediates

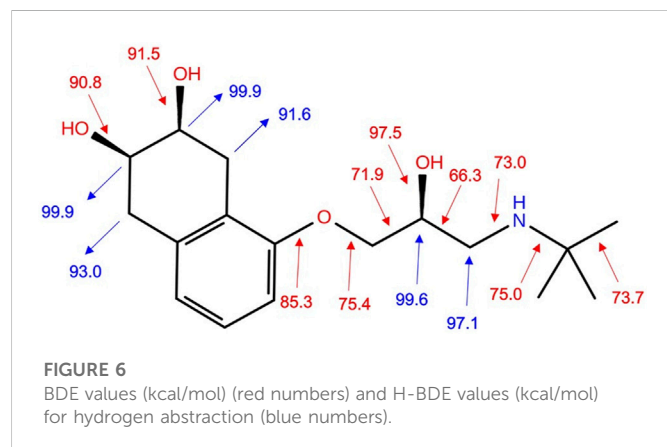
To understand and compare the reactivity of NAD and its photodegradation intermediates, the interaction of NAD and its degradation mixtures with H₂O₂ and free radicals was investigated. The percentage of catalase activity was used to assess the interaction with H₂O₂, the degree of inhibition of lipid peroxidation was used to evaluate the interaction with $\bullet\text{OH}$ radicals, and the degree of hydroxyl radicals neutralization was used to assess the prooxidant or antioxidant activity of obtained degradation mixtures (Figure 3).

In this part of the experiment, catalase activity reflects residual H₂O₂ in the sample mixtures, while the lipid peroxidation process reflects the presence of the intermediates with the potential ability to induce, along with hydroxyl radicals, this process or to reduce it, acting as scavengers of $\bullet\text{OH}$ radicals. Further, the degree of hydroxyl radical neutralization indicates the presence of NAD since it acts as a direct hydroxyl radical scavenger. In comparison to UPW (Figure 3), results suggest that NAD, itself, scavenges $\bullet\text{OH}$ radicals (8% vs. 22%), while the catalase activity and lipid peroxidation process have insignificant influence. Among three indirect photolysis groups, solar radiation produces the smallest amount of hydroxyl radical based on the results of CAT activity. In this group, during the incubation period, an enzyme in the blood was involved in the decomposition of H₂O₂, and as a consequence, its activity was lowest at the end of it. Our assumption is that indirect photolysis with simulated solar radiation induces degradation of NAD in the manner that degradation intermediates exert antioxidant effects since the lipid peroxidation process is drastically decreased (-21%), while the scavenging ability of $\bullet\text{OH}$ radical increased in comparison to UPW and NAD group (37% in comparison to 8% for UPW, and 22% for NAD group). Contrarily, UV-LED and UV indirect photolysis induce the conversion of H₂O₂ to hydroxyl radicals since CAT activity is near the level of UPW (9% and 0%, respectively). Additionally, during the process of NAD degradation, prooxidant intermediates are formed, in contrast to SS indirect photolysis, since the lipid peroxidation process is more than pronounced (32% and 56%). Comparing the results of UV-LED and UV indirect photolysis, our assumption is that there is a slight difference in the degradation path of NAD. Namely, our assumption is that UV induces more prooxidant intermediates able to scavenge $\bullet\text{OH}$ radicals than UV-LED, while UV-LED induced photolysis induces additional antioxidant intermediates since the degree of hydroxyl radical neutralization is higher (11% versus 29%).

In this work impact of NAD (Figure 4) and mixtures formed during indirect photolysis on the growth of human cell lines HT-29 and MRC-5 was assessed *in vitro*. The obtained results depended on the cell line and the type of applied radiation. *In vitro* bioassays using mammalian cell lines can reveal the combined effect of interacting chemical compounds and complex mixtures found in environmental

TABLE 1 Optimized geometries* of the NAD/•OH system with the binding energy and shortest distances between NAD and •OH.

Optimized geometries	1	2	3	4	5	6	7	8	9	10
Binding energy [kcal/mol]	-5.01	-20.59	-11.30	-7.74	-8.26	-10.26	-8.73	/	/	/
Atoms with the shortest distance between NAD and •OH	O50	O50	O50	O19	O50	O21	O1	/	/	/
	I	I	I	I	I	I	I			
	H42	H23	C13	H51	C16	H2	H51			
The shortest distance (Å)	2.602	1.644	2.504	1.848	2.494	1.796	1.896	/	/	/

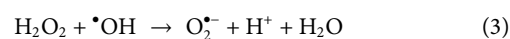
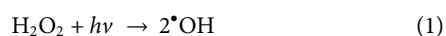


samples and their potential additive, synergistic, or antagonistic effects. Mammalian cell lines are potent tools for predicting the toxicity of a single compound or a mixture of compounds towards higher trophic levels organisms and their organ-specific effects (Četojević-Simin et al., 2013).

A comparison of the *in vitro* toxicity of NAD and evolution of its degradation mixtures obtained under different irradiation types revealed mild cell growth stimulation (<4%) of fetal lung cells MRC-5 and mild to moderate (2%–19%) cell growth stimulation of colon adenocarcinoma cells HT-29. Both parent compound NAD and mixtures obtained after UV/H₂O₂ treatment revealed similar cell growth stimulation patterns in both cell lines, indicating no change in the cell growth effects after irradiation treatment compared to the parent compound. On the other hand, after treatment with UV-LED/H₂O₂ obtained mixture had minimal effect on the growth of both selected cell lines, indicating the evolution of non-toxic intermediates.

3.3 Tentative degradation mechanism of nadolol and its degradation intermediates

A reaction mechanism is a microscopic path by which reactants are transformed into products. Therefore, it is crucial to identify intermediates formed by NAD degradation. The experiments have shown that using UV/H₂O₂ leads to higher degradation efficiency due to the generation of reactive species (reactions 1-3) (Oancea and Meltzer, 2014).



According to literature data, reactive oxygen radicals (•OH and O₂^{•-}) significantly influence the decomposition of organic compounds (Liu et al., 2018). As mentioned in the previous papers (Cai et al., 2022a; Cai et al., 2022b; Li et al., 2022b), different radical scavengers (methanol, benzoic acid, *tert*-butanol, furfuryl alcohol) could be used for identification of generated reactive radicals. IPA and BQ were chosen as •OH and O₂^{•-} scavengers because of the elevated reactivity of IPA with •OH (2×10⁹ L/(mol×s)) (Vione et al., 2010) and BQ with O₂^{•-} (1.1×10⁹ L/(mol×s)) (Zhu et al., 2020), respectively. When these reactive radical scavengers are present, the efficiency of NAD degradation decreases significantly, which indicates that the mechanism of degradation of the investigated compound takes place efficiently precisely in the presence of the mentioned reactive species.

To investigate the influence of •OH and superoxide radicals O₂^{•-} on NAD suspensions, we have added IPA or BQ. As shown in Figure 5, the degradation efficiency of IPA quenching decreased more than that of BQ. After 180 min of degradation, 70% and 20% NAD was less degraded in the presence of IPA and BQ scavengers, respectively. O₂^{•-} is an essential component in many chemical processes (Hayyan et al., 2016), but indirect photolysis of NAD has the lowest impact on its degradation.

To better understand the interaction between NAD and •OH radicals, we conducted a DFT computational analysis of the NAD/•OH system. Ten configurations were obtained (Supplementary Figure S2) by optimizing the investigated system's molecular geometry, which, together with the distance between certain atoms, are given in Table 1. The different location of the •OH radical concerning the NAD molecule indicates other interactions that can take place between them. Namely, it is known that the •OH radical reacts with organic molecules by either adding to unsaturated bonds or hydrogen abstraction (Panchenko, 2006). Since in configurations 3 and 5, the shortest distance of NAD and •OH radicals is between the oxygen atom of the •OH radical and the unsaturated carbons of the NAD ring (C13 and C16, respectively), the mechanism of addition of •OH radical to unsaturated bonds can be assumed.

On the other hand, in configuration 2 the •OH radical is closest to the hydrogen from the aliphatic chain, and in configurations 1, 4, 6, and 7, to the ring, which would mean that abstraction of those hydrogens atoms could occur. From the above, it can be assumed that the primary reaction mechanism in the observed system is hydrogen abstraction. For configurations 8, 9, and 10, it is interesting to note that •OH radical abstracted a hydrogen atom

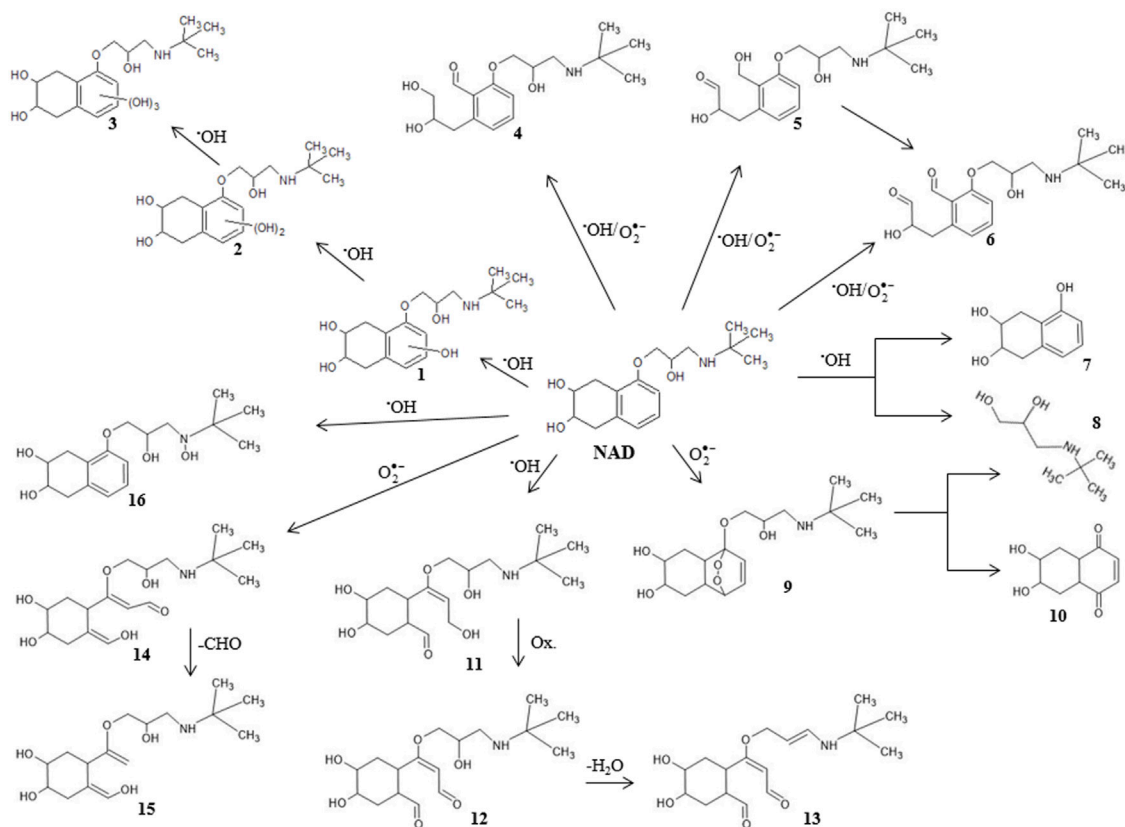


FIGURE 7

Proposal tentative degradation pathways of NAD during UV/H₂O₂ process; Ox.—oxidation.

connected to the nitrogen atom bonded, whereby a water molecule is formed.

In terms of the suggestion of tentative degradation intermediates and predicting sensitivity towards autoxidation, bond dissociation energy for single acyclic bonds (BDE) and for hydrogen abstraction (H-BDE) are shown to be very useful. Namely, the H-BDE values in the range of 70–85 kcal/mol indicate high sensitivity towards autoxidation, and H-BDE values in the range of 85–90 kcal/mol also indicate sensitivity towards autoxidation but must be taken with caution (Lienard et al., 2015; Wright et al., 2009; Gryn'ova et al., 2011). BDE and H-BDE values are reported in Figure 6. H-BDE values indicate that NAD is not sensitive toward autoxidation. It can be presumed that NAD degradation could begin with the detachment of the -R group from the oxygen atom on the tetrahydronaphthalene ring. BDE values of C-C bonds in the NAD aliphatic chain (Figure 6) show that degradation could be continued by breaking these bonds. The bonds connecting the -OR group to the tetrahydronaphthalene ring and the C-OH bonds have the highest calculated BDE values. It was assumed that these bonds hardly break.

According to the obtained results, the formation of intermediates 1, 2, and three was proposed due to the addition of •OH radicals to the NAD ring. On the other hand, it was shown that there is the possibility of abstraction of hydrogen atoms by •OH radicals (Table 1). This mechanism could lead to the formation of NAD radical, which could further react with •OH and O₂^{•-}. In the presence

of identified radicals, the ring opening mechanism is possible, so the appearance of the intermediates from 4 to 6 and from 8 to 15 is suggested. Liu and Williams (2007) proposed three major propranolol photodegradation products due to ring oxidation in the presence of oxygen. Since NAD and propranolol are the most structurally similar β-blockers (both have two rings), it can be assumed that they will have similar degradation pathways during photodegradation (intermediates 14 and 15). Uwai et al. (2005) suggested the oxidation of the propranolol aromatic ring and the aliphatic separation part of molecules. A similar could be recommended for NAD. As stated above, intermediates 8, 9, and 10 are presented in Figure 7. Yang et al. (2010) gave a general scheme for the photodegradation of β-blockers in water in which cleavage of the side chain can also occur in the presence of •OH radicals. Accordingly, the reaction of •OH radicals with NAD leads to the formation of intermediates 7 and 8. BDE values also go in favor of formation intermediates 7 and 8. Also, intermediates 11, 12, 13, and 16 were proposed.

4 Conclusion

This study showed that direct photolysis of NAD under different radiation types had negligible degradation efficiency, whereby UV radiation's degradation efficiency was the highest. The presence of H₂O₂ increased the degradation efficiency under all three types of

irradiation, where 4.5%, 23.1%, and 80.2% of NAD were degraded under SS, UV-LED, and UV radiation after 180 min, respectively. The degree of mineralization was determined after indirect photolysis for all three types of radiation. After 180 min of UV irradiation, only 22.2% of NAD and its intermediates mixture were mineralized. The catalase activity, the degree of inhibition of lipid peroxidation, and the degree of lipid peroxidation were used to assess the reactivity of NAD and its photodegradation intermediates with H_2O_2 . The toxicities of NAD photodegradation mixtures toward human cell lines MRC-5 and HT-29 were investigated. UV-LED/ H_2O_2 treatment produced degradation mixtures with minimal effect on the growth of both selected cell lines. In contrast, UV/ H_2O_2 treatment produced mixtures that had a similar, proliferative effect on cell growth as the parent compound NAD. The influence of reactive oxygen species ($\cdot\text{OH}$ and $\text{O}_2^{\cdot-}$) was investigated by monitoring the efficiency of NAD degradation in the presence of radical scavengers (IPA and BQ) in the UV/ H_2O_2 system. The results show that the influence of these radicals in the degradation of NAD decreases in the order $\cdot\text{OH} > \text{O}_2^{\cdot-}$. Based on the DFT calculations, it can be concluded that NAD is stable toward autoxidation. Also, computational analysis of the NAD/ $\cdot\text{OH}$ system confirms the possibility of interaction between NAD and $\cdot\text{OH}$ radicals. Based on literature data and obtained results, 16 tentative NAD degradation intermediates were proposed. The NMR chemical shifts of the proposed intermediates were given using DFT calculations (Supplementary Material Table S3a-p).

Data availability statement

The raw data supporting the conclusion of this article will be made available by the authors, without undue reservation.

Author contributions

The first draft of the manuscript was written by AB and all authors commented on previous versions of the manuscript. All authors read and approved the final manuscript.

References

- Armaković, S., and Armaković, S. J. (2022). Atomistica.online – web application for generating input files for ORCA molecular modelling package made with the Anvil platform. *Mol. Simul.* 49, 117–123. doi:10.1080/08927022.2022.2126865
- Bannwarth, C., Caldeweyher, E., Ehlert, S., Hansen, A., Pracht, P., Seibert, J., et al. (2021). Extended tight-binding quantum chemistry methods. *WIREs Comput. Mol. Sci.* 1, e1493. doi:10.1002/wcms.1493
- Bannwarth, C., Ehlert, S., and Grimme, S. (2019). GFN2-xTB-An accurate and broadly parametrized self-consistent tight-binding quantum chemical method with multipole electrostatics and density-dependent dispersion contributions. *J. Chem. Theory Comput.* 15 (3), 1652–1671. doi:10.1021/acs.jctc.8b01176
- Becke, A. D. (1993). Density-functional thermochemistry. III. The role of exact exchange. *J. Chem. Phys.* 98, 5648–5652. doi:10.1063/1.464913
- Bochevarov, A. D., Harder, E., Hughes, T. F., Greenwood, J. R., Braden, D. A., and Philipp, D. M., (2013). Jaguar: A high-performance quantum chemistry software program with strengths in life and materials sciences. *Int. J. Quantum Chem.* 113, 2110–2142. doi:10.1002/qua.24481
- Bonvin, F., Omlin, J., Rutler, R., Schweizer, W. B., Alaimo, P. J., and Strathmann, T. J., (2013). Direct photolysis of human metabolites of the antibiotic sulfamethoxazole: Evidence for abiotic back-transformation. *Environ. Sci. Technol.* 47, 6746–6755. doi:10.1021/es303777k
- Cai, H., Zou, J., Lin, J., Li, J., Huang, Y., and Zhang, S., (2022a). Sodium hydroxide-enhanced acetaminophen elimination in heat/peroxymonosulfate system: Production of singlet oxygen and hydroxyl radical. *Chem. Eng. J.* 429, 132438. doi:10.1016/j.cej.2021.132438
- Cai, H., Zou, J., Lin, J., Li, Q., Li, J., and Huang, Y., (2022b). Elimination of acetaminophen in sodium carbonate-enhanced thermal/peroxymonosulfate process: Performances, influencing factors and mechanism. *Chem. Eng. J.* 449, 137765. doi:10.1016/j.cej.2022.137765
- Cao, Y., Beachy, M. D., Braden, D. A., Morrill, L. A., Ringnald, M. N., and Friesner, R. A. (2005). Nuclear-magnetic-resonance shielding constants calculated by pseudospectral methods. *J. Chem. Phys.* 122 (22), 224116. doi:10.1063/1.1924598
- Cao, Y., Halls, M. D., Vadicherla, T. R., and Friesner, R. A. (2021). Pseudospectral implementations of long-range corrected density functional theory. *J. Comput. Chem.* 42, 2089–2102. doi:10.1002/jcc.26739
- Cao, Y., Hughes, T., Giesen, D., Halls, M. D., Goldberg, A., and Vadicherla, T. R., (2016). Highly efficient implementation of pseudospectral time-dependent density-functional theory for the calculation of excitation energies of large molecules. *J. Comput. Chem.* 37, 1425–1441. doi:10.1002/jcc.24350
- Carlson, J. C., Stefan, M. I., Parnis, J. M., and Metcalfe, C. D. (2015). Direct UV photolysis of selected pharmaceuticals, personal care products and endocrine disruptors in aqueous solution. *Water Res.* 84, 350–361. doi:10.1016/j.watres.2015.04.013
- Četojević-Simin, D. D., Armaković, S. J., Šojić, D. V., and Abramović, B. F. (2013). Toxicity assessment of metoprolol and its photodegradation mixtures obtained by using different type of TiO_2 catalysts in the mammalian cell lines. *Sci. Total Environ.* 463–469, 968–974. doi:10.1016/j.scitotenv.2013.06.083
- Ditchfield, R., Hehre, W. J., and Pople, J. A. (1971). Self-consistent molecular-orbital methods. IX. An extended Gaussian-type basis for molecular-orbital studies of organic molecules. *J. Chem. Phys.* 54, 724–728. doi:10.1063/1.1674902

Funding

This research was funded by the Ministry of Education, Science and Technological Development of the Republic of Serbia (Grant No. 451-03-68/2022-14/200125).

Acknowledgments

SJA, SA, and MMS thank the Association for the International Development of Academic and Scientific Collaboration (www.aidasco.org) for providing computational resources necessary for the first principles calculations.

Conflict of interest

The authors declare that the research was conducted in the absence of any commercial or financial relationships that could be construed as a potential conflict of interest.

Publisher's note

All claims expressed in this article are solely those of the authors and do not necessarily represent those of their affiliated organizations, or those of the publisher, the editors and the reviewers. Any product that may be evaluated in this article, or claim that may be made by its manufacturer, is not guaranteed or endorsed by the publisher.

Supplementary material

The Supplementary Material for this article can be found online at: <https://www.frontiersin.org/articles/10.3389/fenvs.2023.1119944/full#supplementary-material>

- Ehlert, S., Stahn, M., and Spicher, S. (2021). Grimme, Robust and Efficient Implicit Solvation Model for Fast Semiempirical Methods. *J. Chem. Theory Comput.* 17, 4250–4261. doi:10.1021/acs.jctc.1c00471
- Fujioka, T., Kodamatani, H., Yoshikawa, T., Inoue, D., and Ikehata, K. (2020). Assessment of 265-nm UV-LED for direct photolysis and advanced oxidation of N-nitrosamines and 1,4-dioxane. *Environ. Technol. Innov* 20, 101147. doi:10.1016/j.eti.2020.101147
- Ghanbari, F., Yaghoob-Nezhad, A., Waclawek, S., Lin, K. A., Rodríguez-Chueca, J., and Mehdipour, F. (2021). Comparative investigation of acetaminophen degradation in aqueous solution by UV/Chlorine and UV/H₂O₂ processes: Kinetics and toxicity assessment, process feasibility and products identification. *Chemosphere* 285, 131455. doi:10.1016/j.chemosphere.2021.131455
- Gomes, A. I., Soares, T. F., Silva, T. F. C. V., Boaventura, R. A. R., and Vilar, V. J. P. (2020). Ozone-driven processes for mature urban landfill leachate treatment: Organic matter degradation, biodegradability enhancement and treatment costs for different reactors configuration. *Sci. Total Environ* 724, 138083. doi:10.1016/j.scitotenv.2020.138083
- Goyal, R., Singh, O., Agrawal, A., Samanta, C., and Sarkar, B. (2020). Advantages and limitations of catalytic oxidation with hydrogen peroxide: From bulk chemicals to lab scale process. *Catal. Rev* 64, 229–285. doi:10.1080/01614940.2020.1796190
- Grimme, S., Bannwarth, C., and Shushkov, P. (2017). A Robust and accurate tight-binding quantum chemical method for structures, vibrational frequencies, and noncovalent interactions of large molecular systems parametrized for All spd-block elements (Z = 1–86). *J. Chem. Theory Comput.* 13 (5), 1989–2000. doi:10.1021/acs.jctc.7b00118
- Gryn'ova, G., Hodgson, J. L., and Coote, M. L. (2011). Revising the mechanism of polymer autooxidation. *Org. Biomol. Chem* 9, 480–490. doi:10.1039/C0OB00596G
- Guo, Z., Kodikara, D., Albi, L. S., Hatano, Y., Chen, G., and Yoshimura, C., (2022). Photodegradation of organic micropollutants in aquatic environment: Importance, factors and processes. *Water Res* 2022, 118236. doi:10.1016/j.watres.2022.118236
- Hayyan, M., Hashim, M. A., and AlNashef, I. M. (2016). Superoxide ion: Generation and chemical implications. *Chem. Rev* 116, 3029–3085. doi:10.1021/acs.chemrev.5b00407
- Jacobson, L. D., Bochevarov, A. D., Watson, M. A., Hughes, T. F., Rinaldo, D., and Ehrlich, S., (2017). Automated transition state search and its application to diverse types of organic reactions. *J. Chem. Theory Comput* 13, 5780–5797. doi:10.1021/acs.jctc.7b00764
- Jelić, M., Mandić, A., Kladar, N., Sudji, J., Božin, B., and Srdjenovic, B. (2018). Lipid peroxidation, antioxidative defense and level of 8-hydroxy-2-deoxyguanosine in cervical cancer patients. *J. Med. Biochem* 37, 336–345. doi:10.1515/jomb-2017-0053
- Khasawneh, O. F. S., and Palaniandy, P. (2021). Occurrence and removal of pharmaceuticals in wastewater treatment plants. *Process Saf. Environ. Prot* 150, 532–556. doi:10.1016/j.psep.2021.04.045
- Khorsandi, H., Teymori, M., Aghapour, A. A., Jafari, S. J., Taghipour, S., and Bargeshadi, R. (2019). Photodegradation of ceftriaxone in aqueous solution by using UVC and UVC/H₂O₂ oxidation processes. *Appl. Water Sci* 9, 81–88. doi:10.1007/s13201-019-0964-2
- Khoschorur, G. A., Winkhofer-Roob, B. M., Rabl, H., Auer, Th., Peng, Z., and Schaur, R. J. (2000). Evaluation of a sensitive HPLC method for the determination of malondialdehyde, and application of the method to different biological materials. *Chromatographia* 52, 181–184. doi:10.1007/BF02490453
- Kladar, N., Srdjenović, B., Grujić, N., Bokić, B., Rat, M., and Anačkov, G., (2015). Ecologically and ontogenetically induced variations in phenolic compounds and biological activities of *Hypericum maculatum* subsp. *maculatum*, *Hypericaceae*. *Braz. J. Bot* 38, 703–715. doi:10.1007/s40415-015-0177-3
- Lee, C., Yang, W., and Parr, R. G. (1988). Development of the Colle-Salvetti correlation-energy formula into a functional of the electron density. *Phys. Rev. B* 37, 785–789. doi:10.1103/physrevb.37.785
- Li et al., 2022aLi, S., Yang, Y., Zheng, H., Zheng, Y., and Jing, T., (2022). Advanced oxidation process based on hydroxyl and sulfate radicals to degrade refractory organic pollutants in landfill leachate. *Chemosphere* 297, 134214. doi:10.1016/j.chemosphere.2022.134214
- Li et al., 2022bLi, J., Zou, J., Zhang, S., Cai, H., and Huang, Y., (2022). Sodium tetraborate simultaneously enhances the degradation of acetaminophen and reduces the formation potential of chlorinated by-products with heat-activated peroxymonosulfate oxidation. *Water Res* 224, 119095. doi:10.1016/j.watres.2022.119095
- Lienard, P., Gavartin, J., Boccardi, G., and Meunier, M. (2015). Predicting drug substances autooxidation. *Pharm. Res* 32, 300–310. doi:10.1007/s11095-014-1463-7
- Liu, J., Zhang, P., Tian, Z., Xu, R., Wu, Y., and Song, Y. (2020). Pollutant removal from landfill leachate via two-stage anoxic/oxic combined membrane bioreactor: Insight in organic characteristics and predictive function analysis of nitrogen-removal bacteria. *Bioresour. Technol* 317, 124037. doi:10.1016/j.biortech.2020.124037
- Liu, Q.-T., and Williams, H. E. (2007). Kinetics and degradation products for direct photolysis of β -blockers in water. *Environ. Sci. Technol* 41, 803–810. doi:10.1021/es0616130
- Liu, T., Yin, K., Liu, C., Luo, J., Crittenden, J., and Zhang, W., (2018). The role of reactive oxygen species and carbonate radical in oxcarbazepine degradation via UV, UV/H₂O₂: Kinetics, mechanisms and toxicity evaluation. *Water Res* 147, 204–213. doi:10.1016/j.watres.2018.10.007
- Lopez-Alvarez, B., Villegas-Guzman, P., Penuela, G. A., and Torres-Palma, R. A. (2016). Degradation of a toxic mixture of the pesticides carbofuran and iprodione by UV/H₂O₂: Evaluation of parameters and implications of the degradation pathways on the synergistic effects. *Wat. Air Soil Poll* 227, 215. doi:10.1007/s11270-016-2903-2
- Maszkowska, J., Stolte, S., Kumsirka, J., Łukaszewicz, P., Mioduszczyńska, K., and Puckowski, A., (2014). Beta-blockers in the environment: Part I. Mobility and hydrolysis study. *Sci. Total Environ* 493, 1112–1121. doi:10.1016/j.scitotenv.2014.06.023
- Oancea, P., and Meltzer, V. (2014). Kinetics of tartrazine photodegradation by UV/H₂O₂ in aqueous solution. *Chem. Pap* 68, 105–111. doi:10.2478/s11696-013-0426-5
- Panchenko, A. (2006). DFT investigation of the polymer electrolyte membrane degradation caused by OH radicals in fuel cells. *J. Membr. Sci* 278, 269–278. doi:10.1016/j.memsci.2005.11.010
- Piram, A., S. A., Verne, C., Herbreteau, B., and Faure, R. (2008). Photolysis of β -blockers in environmental waters. *Chemosphere* 73, 1265–1271. doi:10.1016/j.chemosphere.2008.07.018
- Pracht, P., Caldeweyher, E., Ehlert, S., and Grimme, S. (2019). A robust non-self-consistent tight-binding quantum chemistry method for large molecules. *ChemRxiv* [Preprint]. doi:10.26434/chemrxiv.8326202
- Rassolov, V. A., Pople, J. A., Ratner, M. A., and Windus, T. L. (1998). 6-31G* basis set for atoms K through Zn. *J. Chem. Phys* 109, 1223–1229. doi:10.1063/1.476673
- Rassolov, V. A., Ratner, M. A., Pople, J. A., Redfern, P. C., and Curtiss, L. A. (2001). 6-31G* basis set for third-row atoms. *J. Comput. Chem* 22, 976–984. doi:10.1002/jcc.1058
- Santolin, V., Tochetto, G. A., Dervanoski, A., and Pasquali, G. D. L. (2022). Optimization of p-nitrophenol degradation and mineralization using a photochemical reactor. *Wat. Air Soil Poll* 233, 242. doi:10.1007/s11270-022-05740-4
- Skehan, P., Storeng, R., Scudiero, D., Monks, A., McMahon, J., and Vistica, D., (1990). New colorimetric cytotoxicity assay for anticancer-drug screening. *J. Natl. Cancer. Inst* 82, 1107–1112. doi:10.1093/jnci/82.13.1107
- Stephens, P. J., Devlin, F. J., Chabalowski, C. F., and Frisch, M. J. (1994). *Ab initio* calculation of vibrational absorption and circular dichroism spectra using density functional force fields. *J. Phys. Chem* 98, 11623–11627. doi:10.1021/j100096a001
- Svendsen, S. B., El-taliawy, H., Carvalho, P. N., and Bester, K. (2020). Concentration dependent degradation of pharmaceuticals in WWTP effluent by biofilm reactors. *Water Res* 186, 116389. doi:10.1016/j.watres.2020.116389
- Uwai, K., Tani, M., Ohtake, Y., Abe, S., Maruko, A., and Chiba, T., (2005). Photodegradation products of propranolol: The structures and pharmacological studies. *Life Sci* 78, 357–365. doi:10.1016/j.lfs.2005.04.033
- Vione, D., Khanra, S., Das, R., Minerio, C., Maurino, V., and Brigante, M., (2010). Effect of dissolved organic compounds on the photodegradation of the herbicide MCPA in aqueous solution. *Water Res* 44, 6053–6062. doi:10.1016/j.watres.2010.07.079
- Vosko, S. H., Wilk, L., and Nusair, M. (1980). Accurate spin-dependent electron liquid correlation energies for local spin density calculations: A critical analysis. *Can. J. Phys* 58, 1200–1211. doi:10.1139/p80-159
- Wang, L., Xu, H., Cooper, W. J., and Song, W. (2012). Photochemical fate of beta-blockers in NOM enriched waters. *Sci. Total Environ* 426, 289–295. doi:10.1016/j.scitotenv.2012.03.031
- Wols, B. A., Hofman-Caris, C. H. M., Harmsen, D. J. H., and Beerendonk, E. F. (2013). Degradation of 40 selected pharmaceuticals by UV/H₂O₂. *Water Res* 47, 5876–5888. doi:10.1016/j.watres.2013.07.008
- Wright, J. S., Shadnia, H., and Chepelev, L. L. (2009). Stability of carbon-centered radicals: Effect of functional groups on the energetics of addition of molecular oxygen. *J. Comput. Chem* 30, 1016–1026. doi:10.1002/jcc.21124
- Yang, H., Ana, T., Li, G., Song, W., Cooper, W., and Luo, H., (2010). Photocatalytic degradation kinetics and mechanism of environmental pharmaceuticals in aqueous suspension of TiO₂: A case of β blockers. *J. Hazard. Mater* 179, 834–839. doi:10.1016/j.jhazmat.2010.03.079
- Ye, Z., Guo, Z., Wang, J., Zhang, L., Guo, Y., Yoshimura, C., et al. (2022). Photodegradation of acebutolol in natural waters: Important roles of carbonate radical and hydroxyl radical. *Chemosphere* 287, 132318. doi:10.1016/j.chemosphere.2021.132318
- Yi, M., Sheng, Q., Sui, Q., and Lu, H. (2020). β -blockers in the environment: Distribution, transformation, and ecotoxicity. *Environ. Pollut* 266, 115269. doi:10.1016/j.envpol.2020.115269
- Zhan, M.-X., Liu, Y.-W., Ye, W.-W., and Jiao, T. C., and (2022). Modification of activated carbon using urea to enhance the adsorption of dioxins. *Environ. Res* 204, 112035. doi:10.1016/j.envres.2021.112035
- Zhu, M., Lu, J., Hu, Y., Liu, Y., Hu, S., and Zhu, C. (2020). Photochemical reactions between 1,4-benzoquinone and O₂^{•-}. *Environ. Sci. Pollut. Res* 27, 31289–31299. doi:10.1007/s11356-020-09422-8